

## An improved algorithm for the shape from shading problem\*

ROBERT T. FRANKOT<sup>†</sup>

Hughes Aircraft Company, Radar Systems Group, El Segundo, California, USA.

AND

RAMA CHELLAPPA<sup>‡</sup>

Signal and Image Processing Institute, University of Southern California, Department of EE-Systems, Los Angeles, California, USA 90089.

### Abstract

Recently developed techniques for estimating surface shape from shading information suffer from the following drawback: Surface slopes are estimated without ensuring that those slopes correspond to a valid surface. In this paper, an existing iterative algorithm is improved by projecting the surface slope estimates on to a valid set of surface slopes at each iteration. Specifically, we require that the second partial derivatives of the surface do not depend on the order in which differentiation is performed. The result is a more stable shape from shading algorithm with a reduction in sensitivity to modeling errors and incomplete boundary conditions. Experimental results are presented for simulated and real images.

**Key words:** Surface shape, shading information.

### 1. Introduction

Shape from shading refers to the problem of determining the shape of a smooth surface given a single image of that surface. One way to infer surface variations given a single image is to model the observed image intensity in terms of the surface slopes and then solve for the surface slopes.

Let  $I(x, y)$  be the observed image intensity and  $z(x, y)$  be the unknown surface height above the  $(x, y)$  plane. We express the relationship between image intensity and surface slopes in the following form<sup>1,2</sup>,

$$I(x, y) = R(z_x, z_y, \beta, l, \rho) \quad (1)$$

where  $z_x = \partial z / \partial x$  and  $z_y = \partial z / \partial y$  are the surface slopes,  $\beta$  the illumination direction vector,  $l$  the vector from the surface to the camera, and  $\rho$  the albedo or intrinsic reflecti-

<sup>†</sup>First presented at the Platinum Jubilee Conference on Systems and Signal Processing held at the Indian Institute of Science, Bangalore, India, during December 11-13, 1986.

<sup>‡</sup>Partially supported by the Hughes Doctoral Fellowship Program.

<sup>‡</sup>Partially supported by the NSF Presidential Young Investigator Award, Under the Grant No. DCI 84-51010 and matching funds from Hughes Aircraft Company, IBM and AT&T.

vity of the materials composing the surface. At any point,  $(x_0, y_0)$ , the reflectance map,  $R$ , is assumed to be a function of the surface slopes and albedo only at  $(x_0, y_0)$ , *i.e.* multiple reflections are ignored. We also assume that the albedo and the vectors  $\beta$  and  $l$  are known over the entire image, and  $R$  is spatially invariant. The imaging geometry is illustrated in fig. 1.

It is apparent from (1) that shape from shading can be expressed as a problem of solving a first-order nonlinear partial differential equation in  $x$  and  $y$ . Early solutions<sup>1-3</sup> were based on direct inversion of the differential equation (1) and served to demonstrate the concept of shape from shading.

Unfortunately, an exact solution to the imaging equation (1) does not always exist, or there may be an infinite number of solutions. In practice, modeling errors such as reflectance map mismatch, imperfect knowledge of the light source, spatial and radiometric quantization error, observation noise, and albedo variations are inevitable. Further, boundary conditions are generally not completely known and sometimes may not be available at all. The existence and uniqueness of a solution to (1) depends on all of these factors. Hence, shape from shading is a very difficult problem in practice.

It is more practical to pose shape from shading as a constrained minimization problem rather than purely an inversion problem. Brooks and Horn<sup>4</sup> proposed the approach of selecting the surface estimate,  $\hat{z}(x, y)$ , which minimizes the following cost function

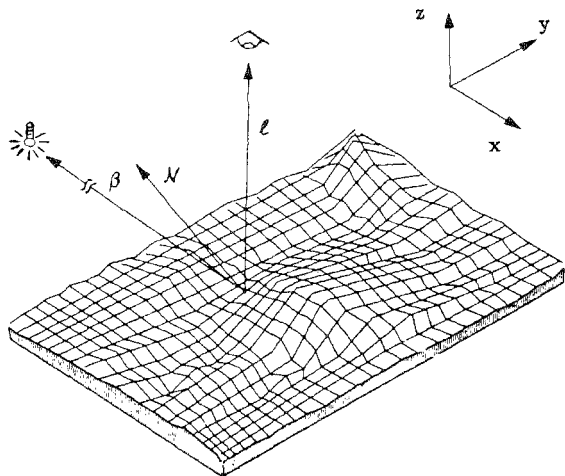


FIG. 1. Imaging geometry.

$$\epsilon = \int \int (I - R(\hat{z}_x, \hat{z}_y))^2 + \lambda \cdot (\hat{z}_{xx}^2 + 2\hat{z}_{xy}^2 + \hat{z}_{yy}^2) dx dy, \quad (2)$$

subject to certain constraints. The first term in the integrand is the squared error between the observed image intensity and the image intensity predicted by substituting the estimates  $(\hat{z}_x, \hat{z}_y)$  into (1). This mean-squared error term allows for modeling errors and noise. The second term in the integrand is a measure of quadratic variation in the surface slopes, with  $\lambda$  constant. This is a smoothness criterion which, in principle, assures a unique smooth solution to (2) even when (1) does not possess a unique solution. It is interesting to note that minimizing quadratic variation of the surface slopes is roughly equivalent to minimizing the potential energy of the surface<sup>5</sup>.

Brooks and Horn<sup>4</sup> developed an algorithm to minimize  $\epsilon$  in (2) subject to the constraint that  $(\hat{z}_x, \hat{z}_y)$  satisfy known boundary conditions. The resulting algorithm yields good results under very limited conditions. The major drawback of the Brooks and Horn algorithm is that it does not take into account the interdependence of the functions  $z_x$  and  $z_y$  but allows them to vary independently. If we allow  $(z_x, z_y)$  to vary independently then (1) may have an infinite number of solutions even when boundary conditions are completely known and there are no modeling errors. Similarly, the local approach developed by Pentland<sup>6</sup> and later improved by Lee and Rosenfeld<sup>7</sup> does not require any sort of global consistency of the slope estimates.

We have developed a simple solution to this problem by requiring that

$$z_{xy}(x, y) = z_{yz}(x, y), \quad (3)$$

for all  $(x, y)$  on the support of  $I$ , that is the second partial derivatives must be independent of the order of differentiation. The only restriction this places on the surface is that  $z(x, y)$  must be twice differentiable, as already assumed in using the cost function (2). Conceptually, this simply enforces one of the basic tenets of the problem formulation. The practical contribution of enforcing (3) is a more stable shape from shading algorithm with a reduction in sensitivity to modeling errors and incomplete boundary conditions.

## 2. Shape from shading algorithm

There are many conceivable ways of enforcing (3). We have developed an approach based on projecting the estimated surface slopes,  $(\hat{z}_x, \hat{z}_y)$ , on to the surface slopes,  $(\bar{z}_x, \bar{z}_y)$ , satisfying (3) while minimizing the following distance measure

$$d\{(\hat{z}_x, \hat{z}_y), (\bar{z}_x, \bar{z}_y)\} = \int \int (\bar{z}_x - \hat{z}_x)^2 + (\bar{z}_y - \hat{z}_y)^2 dx dy. \quad (4)$$

The surface height,  $\bar{z}$ , is represented by a finite sum of orthonormal basis functions satisfying (3) and therefore satisfies (3) also. We have chosen to use the Fourier basis functions  $\{\exp(j\omega_x x + j\omega_y y)\}$ , since they simplify the minimization of (2) and allow efficient computation using fast Fourier transform (FFT) techniques.

Using this approach the surface is represented by

$$\bar{z}(x, y) = \sum_{\omega \in \Omega} \hat{C}(\omega) \exp\{j\omega \cdot (x, y)\} \quad (5)$$

where  $\{\hat{C}\}$  are the coefficients of the Fourier series expansion of  $\hat{z}$ , and  $\underline{\omega} = (w_x, w_y)$  is a two-dimensional index. For images of size  $N$  by  $N$ ,  $\Omega$  is normally  $[0, 1, \dots, N-1] \times [0, 1, \dots, N-1]$  or a subset thereof. Now let  $\hat{C}_x, \hat{C}_y, \tilde{C}_x, \tilde{C}_y$  be the Fourier coefficients for  $\hat{z}_x, \hat{z}_y, \tilde{z}_x, \tilde{z}_y$ , respectively. Then it is straightforward to show that (4) is minimized by taking

$$\tilde{C}(\underline{\omega}) = \frac{-jw_x \hat{C}_x(\underline{\omega}) - jw_y \hat{C}_y(\underline{\omega})}{w_x^2 + w_y^2} \quad (6)$$

with the Fourier coefficients of the constrained surface slopes given by

$$\tilde{C}_x(\underline{\omega}) = jw_x \tilde{C}(\underline{\omega}) \text{ and } \tilde{C}_y(\underline{\omega}) = jw_y \tilde{C}(\underline{\omega}).$$

Now for computer implementation some form of discretization is necessary. For computational simplicity, assume that the surface slopes are circularly periodic and use FFTs to evaluate the Fourier coefficients,  $\hat{C}_x$  and  $\hat{C}_y$ . With this discrete periodic formulation, (4) is minimized by

$$\tilde{C}(\underline{\omega}) = \frac{a_x^*(w_x) \hat{C}_x(\underline{\omega}) + a_y^*(w_y) \hat{C}_y(\underline{\omega})}{|a_x|^2 + |a_y|^2} \quad (7)$$

with

$$\tilde{C}_x(\underline{\omega}) = a_x(w_x) \tilde{C}(\underline{\omega}) \text{ and } \tilde{C}_y(\underline{\omega}) = a_y(w_y) \tilde{C}(\underline{\omega}),$$

where  $a_x$  and  $a_y$  are the Fourier coefficients of the discrete differentiation operators in  $x$  and  $y$ . Suppose we approximate the derivatives by finite central differences, e.g.

$$z_y(l, m) \approx \frac{1}{2} [z(l+1, m) - z(l-1, m)] \quad (8)$$

and similarly for  $z_x$ . For the central difference operator above we get  $a_y(w_y) = \frac{1}{2} \exp\{jw_y\} - \frac{1}{2} \exp\{-jw_y\}$ , and similarly  $a_x(w_x) = \frac{1}{2} \exp\{jw_x\} - \frac{1}{2} \exp\{-jw_x\}$ .

A shape from shading algorithm is now described which minimizes (2) and also satisfies the discrete form of (3) and (4) at each iteration.

Using the finite difference approximations, the values of  $\hat{z}_x(x, y)$  and  $\hat{z}_y(x, y)$  which minimize  $\epsilon$  are found iteratively by the following recursion for each point  $(x, y)$ ,

$$\begin{bmatrix} \hat{z}_x \\ \hat{z}_y \end{bmatrix}_{k+1} = \begin{bmatrix} \hat{z}_x \\ \hat{z}_y \end{bmatrix}_k + \lambda_1 (I - R) \begin{bmatrix} \frac{\partial}{\partial z_x} R \\ \frac{\partial}{\partial z_y} R \end{bmatrix}$$

at the  $(k+1)$ th iteration, where  $R$  and its partials are evaluated at  $[\hat{z}_x, \hat{z}_y]_k$ ,  $\lambda_1$  is a constant inversely proportional to  $\lambda$  in (2),  $[\hat{z}_x, \hat{z}_y]_k$  is a smoothed version of  $[\tilde{z}_x, \tilde{z}_y]_k$ , and  $[\tilde{z}_x, \tilde{z}_y]_k$  is obtained by substituting the raw estimates,  $[\hat{z}_x, \hat{z}_y]_k$ , into (7).

The smoothing applied during each iteration is given by Brooks and Horn<sup>4</sup>

$$\begin{aligned} \hat{z}_y(l, m) = & \frac{1}{5} [\bar{z}_y(l, m+1) + \bar{z}_y(l, m-1) \\ & + \bar{z}_y(l+1, m) + \bar{z}_y(l-1, m)] \\ & + \frac{1}{20} [\bar{z}_y(l-1, m-1) + \bar{z}_y(l-1, m+1) \\ & + \bar{z}_y(l+1, m+1) + \bar{z}_y(l+1, m-1)] \end{aligned} \quad (10)$$

and similarly for  $\hat{z}_x$ . Note that this is just a discrete approximation to the Laplacian with the center pixel left out. The rationale for smoothing  $[\hat{z}_x, \hat{z}_y]_k$  is discussed thoroughly by Ikeuchi and Horn<sup>8</sup> and Brooks and Horn<sup>4</sup>.

The iterative algorithm can be summarized as follows: smooth the previous slope estimates using (10), generate a new set of raw slope estimates using (9), and project the raw slope estimates on to the nearest feasible solution using (7). The process is repeated until the cost function either stops decreasing or becomes sufficiently small. Note that the surface height is obtained by simply performing the inverse DFT of  $\hat{C}(\omega)$  after the final iteration.

### 3. Experimental results

The above algorithm was tested on synthetic imagery with and without known boundary conditions and was also tested on real imagery. Figure 2 shows a partial sphere imbedded in a plane, an image generated from that surface, the surface estimated given both the image intensity and knowledge of the surface slopes around the border of the image, and the estimated surface obtained from the shape from shading algorithm given only the simulated image. This is in contrast with the earlier algorithm in Brooks and Horn<sup>4</sup> which requires knowledge of the slopes where the sphere intersects the plane.

In fig. 3, a picture of the surface of the moon is shown along with a surface estimated based on a guessed light source direction and an assumed reflectance map. Boundary conditions are neither known nor guessed in advance and a reasonable surface estimate is obtained. Finally in fig. 4 predicted images are synthesized for various imaging geometries given only the original sphere and moon images. Here, the shape from shading algorithm is applied to obtain a viewpoint-independent representation of the image.

### 4. Extensions

The algorithm used for enforcing integrability provides an integrator that minimizes the effects of local surface slope errors by combining all of the available data in a globally consistent manner. Therefore, it may also be applied to other computer vision techniques such as shape from texture and Pentland's local shape from shading approach<sup>6</sup>.

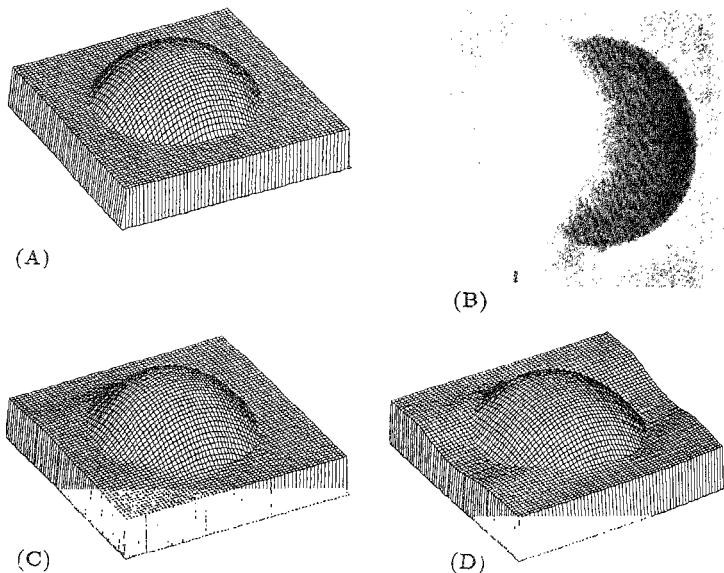


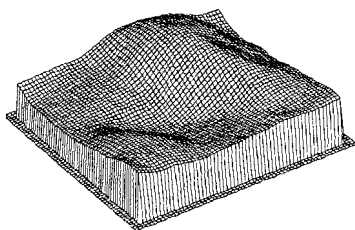
FIG. 2. Shape from shading results using simulated imagery: (A) shows the true surface shape, (B) shows an image simulated from that surface, (C) is the surface estimated by assuming that all surface slopes around the border of the image are zero, (D) is the surface estimated with unknown boundary slopes.

The Fourier transform approach provides an efficient mechanism for including low-resolution information from other sources, such as stereo-image pairs. If a low-resolution surface estimate is indeed available, then the Fourier coefficients of the low-resolution surface are substituted for the low-frequency Fourier coefficients of the shading-based surface reconstruction  $\hat{C}(\omega)$ . This is most useful when complete boundary conditions are not available and in applications where the observed image is noisy. The lowest-frequency components of the surface are lost in the image formation process because image intensity is a function of surface derivatives.

The algorithm presented in this paper has also been extended for application to SAR imagery by using appropriate models for synthetic aperture radar (SAR) image coordinate systems and reflectance maps. SAR image coordinates are approximated by an orthographic projection of the surface height coordinates relative to a plane parallel to the line-of-sight. The shape from shading problem formulation for conventional photographs represents image coordinates as an orthographic projection of the surface height coordinates relative to a plane *orthogonal* to the line-of-sight. Hence, adaptation of the

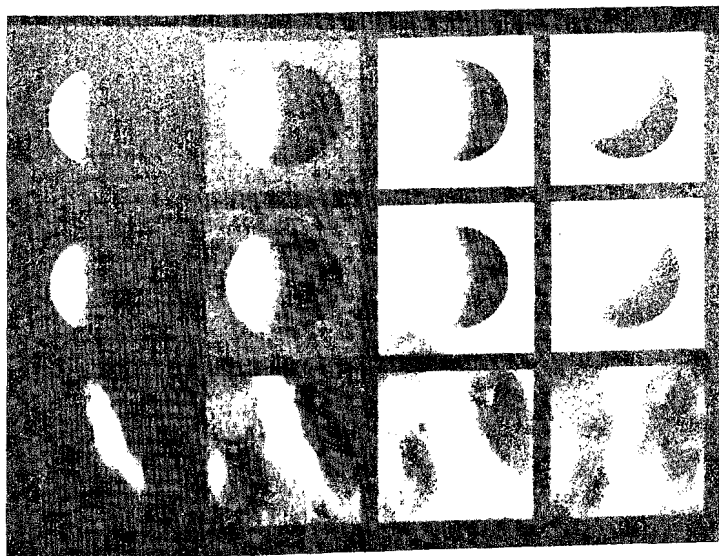


(A)



(B)

FIG.3. Shape from shading results for real imagery of the moon; (A) shows the observed image, and (B) is the estimated surface.



algorithm to the SAR image coordinates is straightforward. The arbitrary reflectance map used in the shape from shading formulation allows us to simply substitute a reflectance model for the SAR imagery. Typical SAR reflectance models have one or more parameters that are not observable given the image intensity alone. When a low-surface estimate is available along with the image intensity it is possible to estimate reflectance map parameters and albedo.

## 5. Conclusions

A previously developed iterative shape from shading algorithm has been improved by strictly enforcing integrability of the surface slopes obtained at each iteration. An efficient computational approach was obtained using fast Fourier transforms. The resulting shape from shading algorithm is more robust than the previous algorithms. It also provides an additional mechanism for including data from other sources. The algorithm is suitable for noisy imagery and has also been extended for application to SAR imagery.

With these developments, shape from shading should find use in some real-world remote-sensing applications. Practical applications for shape from shading are now being examined. Effort is underway to gain a better understanding of the shape from shading problem and to develop further improvements in numerical algorithms for its solution.

## References

1. VAN DIGGELEN, J. A photometric investigation of the slopes and heights of the ranges of hills in the Maria of the Moon, *Bull. Astr. Inst. Ned.*, 1951, 11.
2. HORN, B. K. P. Obtaining shape from shading information, in *The psychology of machine vision*, ed. P. H. Winston, McGraw-Hill, 1975, 115-155.
3. REINDFLEISCH, T. Photometric method for lunar topography, *Photogrammetric Engng.*, 1966, 32, 262-276.
4. BROOKS, M. J. AND HORN, B. K. P. Shape and source from shading, *Proc. Int. Jt Conf. on Artif. Intell.*, Los Angeles, Aug. 1985, pp. 932-936.
5. GRIMSON, W. E. L. *From images to surfaces*, MIT Press, Cambridge, Mass., 1981
6. PENTLAND, A. P. *The visual inference of shape: Computation from local features*. Ph.D. Dissertation, Department of Psychology, MIT, Cambridge, MA, 1982.
7. LEE, C. H. AND ROSENFELD, A. Improved methods of estimating shape from shading using the light source coordinate system, *Artif. Intell.*, 1985, 26, 125-143.
8. IKEUCHI, K. AND HORN, B. K. P. Numerical shape from shading and occluding boundaries, *Artif. Intell.*, 1981, 17, 141-184.

FIG. 4. Predicted images for various imaging geometries given shape from shading results. The first row uses the true sphere surface to predict the images, the second uses only the simulated sphere image from fig. 2, and the third uses only the moon image from fig. 3. The first column is for illumination from the west at  $10^\circ$  above the horizon, the second column has illumination at  $30^\circ$  above the horizon, the third column has illumination at  $45^\circ$  above the horizon, and the fourth column has illumination from the northwest instead of directly from the west.